

Sensing Bandwidth Enlargement with Ten Orthogonal Codes in Quasi-distributed Acoustic Sensing System

Ziwen Deng^a, Ruobing Xu^b, Yuyao Wang^c, Jialin Jiang^d and Zinan Wang^{*e}
Key Lab of Optical Fiber Sensing & Communications, University of Electronic Science and Technology of China,
Chengdu, China

Keywords: Optical Fiber Sensing, Acoustic Sensing, Orthogonal Codes, Sensing Bandwidth, Real-time.

Abstract: In recent years, quasi-distributed acoustic sensing (QDAS) has attracted lots of attentions and shows great advantages in various fields such as structure health monitoring, intrusion sensing and so on. Sensing bandwidth is one of the essential indexes in QDAS, and there is a trade-off between sensing bandwidth and sensing distance. To break the limitation, the multiple-input multiple-output (MIMO) technology and ten orthogonal codes in the same frequency (OCSF) are utilized as an innovative technology to multiplex the sensing channel in a real-time long-distance QDAS system. In this paper, the sensing bandwidth of QDAS is enlarged to 5 kHz on 99.4 km sensing fiber, which is ten times of that in the conventional QDAS without channel multiplexing; a 4.9 kHz sinusoidal signal is retrieved in real time successfully, with 10 m spatial resolution and $43.8 p\epsilon/\sqrt{Hz}$ noise level.

1 INTRODUCTION

With the increasing demand for high-sensitivity acoustic sensing in the fields like railway traffic system supervision, border security, oil and gas monitoring and so on, distributed optical fiber sensing (DOFS) technology is playing an important role in these scenarios. With various advantages, DOFS is a research hot area in recent decades and the further value of it is gradually being explored.

As an important branch of DOFS, phase sensitive optical time domain reflectometry (Φ -OTDR) uses high coherent narrow-linewidth laser as the light source to sense the fluctuation of the external environment through the phase of the Rayleigh backscattering (RBS) light. Φ -OTDR is based on optical fiber to perceive acoustic signal, and it has the merit of high sensitivity, high temperature resistance, anti-corrosion and being immune to electromagnetic interference, so it can be used for tracking the trains and cars, monitoring earthquakes and other important fields.

Φ -OTDR can be divided to distributed acoustic sensing (DAS) and quasi-distributed acoustic sensing (QDAS) according to the different sensing media. DAS is based on common single mode fiber (SMF) and QDAS is based on SMF inscribed with fiber Bragg gratings (FBGs) or scattering enhanced points (SEPs) array.

DAS has the advantages of low cost and flexible spatial resolution. However, the weak and random Rayleigh scattering may cause the fading phenomenon, which need more resources to deal with. While in QDAS, the FBG can offer controllable and stable reflection. Thus, QDAS has higher sensitivity and signal-to-noise ratio (SNR), without fading problem. Due to these advantages, QDAS has developed rapidly and has been a preferred choice in some applications.

In QDAS, the sensing bandwidth is an important parameter and need to be enlarged effectively. By applying Vernier effect in QDAS, the sensing bandwidth can be enlarged to dozens of times, but the target acoustic signal is presupposed to be narrow

^a <https://orcid.org/0000-0003-3198-5423>

^b <https://orcid.org/0000-0001-8510-6135>

^c <https://orcid.org/0000-0002-6846-9089>

^d <https://orcid.org/0000-0001-5354-4157>

^e <https://orcid.org/0000-0002-6924-3428>

band only. Therefore, to avoid limiting the frequency feature of signal, multiplexing the sensing bandwidth is the only way to achieve it. Besides, there is a trade-off between sensing bandwidth and sensing distance, because in QDAS, the sensing signals from different FBGs are distinguished by time of flight. To break the limitations, frequency-division-multiplexing (FDM) is an efficient method, which can multiplex the sensing channel. However, FDM requires extra frequency-domain resources to realize channel-multiplexing, but the frequency-domain resources are precious and supposed to be utilized efficiently.

Recently, our group proposed a QDAS based on multiple-input multiple-output (MIMO) coding technology, which utilized the orthogonal codes in the same frequency (OCSF) to multiplex the sensing channel. The number of the multiplexed sensing channels depend on the number of the groups of the codes used. We utilized sequential quadratic programming (SQP) algorithm to obtain five groups of OCSF with high auto-correlation and cross-correlation suppression ratio, indicating the sensing channels were multiplexed five times and the sensing bandwidth was five times of that in the conventional QDAS.

In this paper, to further enlarge the number of the multiplexed channels, ten codes with about 15.4 dB peak-to-sidelobe ratio of auto-correlation function and cross-correlation are generated, which are the most codes utilized in QDAS. The spatial resolution is determined by the interval of FBGs, i.e. 10 m. By utilizing the OCSF and the MIMO technology, the sensing bandwidth is enlarged to ten times of that in the conventional QDAS without channel-multiplexing. Furthermore, a 1455 nm Raman pump is used for distributed amplification to achieve the long-distance fiber sensing. Moreover, by utilizing GPU parallel processing, the disturbance can be demodulated in real time. As a result, a 5 kHz sensing bandwidth is achieved on a 99.4 km fiber, and the external disturbance, can be retrieved real-time successfully with about 20.5 dB SNR and the strain noise level of $43.8 \text{ } \mu\epsilon/\sqrt{\text{Hz}}$.

2 PRINCIPLES

2.1 The Sensing Principle of QDAS

In QDAS, the sensing fiber is an SMF with a series of enhanced points, which are consist of FBGs/SEPs, whose reflectivity is much higher than the Rayleigh scattering (RS).

The light source is modulated into probe pulses and then injected into the sensing fiber. The lightwaves will be reflected by the enhanced points, and the speckled trace is obtained. When a perturbation, usually acoustic wave, is imposed on the sensing fiber, the optical path experienced by the probe lightwaves will be changed. Therefore, the perturbation can be retrieved and its position can be located by calculating the phase difference of the adjacent signals and the time of flight.

To introduce the MIMO-QDAS, the sensing probe pulse $P(t)$ is coded by M groups of OCSF each with N bits length. The amplitudes of OCSF are the same but the phases are different. The reflected lightwave $E(t)$ can be expressed as:

$$E(t) = h(t) * \sum_{i=1}^M P^i(t - iT_r / M) \quad (1)$$

$$P^i(t) = p^i(t) \cdot \exp(j2\pi f_c t) \quad (2)$$

where $h(t)$ is the impulse response of the sensing fiber; T_r is the repeat period of the lightwave; $p^i(t)$ is the i^{th} modulation function of the probe pulse; M is the number of dimensions of OCSF and f_c is the frequency of optical carrier.

After detecting by coherent detection, the decoded sensing signal can be expressed as:

$$\begin{aligned} E'(t, i) &= E(t) \otimes p^i(t) \\ &= h(t) * p^i(t - iT_r / M) \otimes p^i(t) \\ &+ \sum_{j=1, \dots, M, j \neq i} h(t) * p^j(t - jT_r / M) \otimes p^i(t) \end{aligned} \quad (3)$$

where $*$ denotes the convolution operation and \otimes means the correlation operation.

Assuming the codes have high peak-to-sidelobe ratio of auto-correlation function and cross-correlation function, then $E'(t, i)$ can be approximated as:

$$E'(t, i) \approx h(t) * P_{main}(t - iT_r / M) \quad (4)$$

where P_{main} denotes the main lobe of the auto-correlation function of $p^i(t)$.

Eq. (4) shows that the sensing channel probed by the pulse P_{main} with a repetition period of T_r / M is extracted. Therefore, the disturbance sampling rate is increased by M times and the OCSF need no extra frequency band for multiplexing. The acoustic signal can be demodulated by demodulating the phase information, demonstrating that the sensing channel

has been multiplexed M times and the sensing bandwidth is enhanced M times of that in the conventional QDAS without channel-multiplexing.

2.2 the Generation of Codes

According to Eq. (3), the OCSF are supposed to be with high peak-to-sidelobe ratio of auto-correlation function and cross-correlation function, so that the equation can be approximated as Eq. (4).

To obtain the required codes is an optimization problem, and the objective function and constraint condition are given by:

$$\begin{aligned}
 & \min_{A,C,\varphi,t} t \\
 & s.t. \quad |A(m,k)| - t \leq 0, \\
 & \quad m=1 \cdots M, k=-N+1 \cdots N-1, k \neq 0; \\
 & \quad |C(m,n,k)| - t \leq 0, \\
 & \quad m,n=1 \cdots M, k=-N+1 \cdots N-1, m \neq n; \\
 & \quad 0 \leq |A| \leq 1; \\
 & \quad 0 \leq \varphi \leq 2\pi;
 \end{aligned} \tag{5}$$

where N is the code length; $A(m,k)$ is the k^{th} value of the auto-correlation function of the m^{th} code; $C(m,n,k)$ is the k^{th} value of the cross-correlation function of the m^{th} code and the n^{th} code; $|A|$ represents the amplitudes of the codes, which is a $M \times (2N-1)$ matrix and φ means the phases of the codes, which is a $M \times N$ matrix.

The amplitudes of the OCSF are the same, but the phases of them are different, which range from 0 to 2π . The optimization problem above can be solved by sequential quadratic programming (SQP)

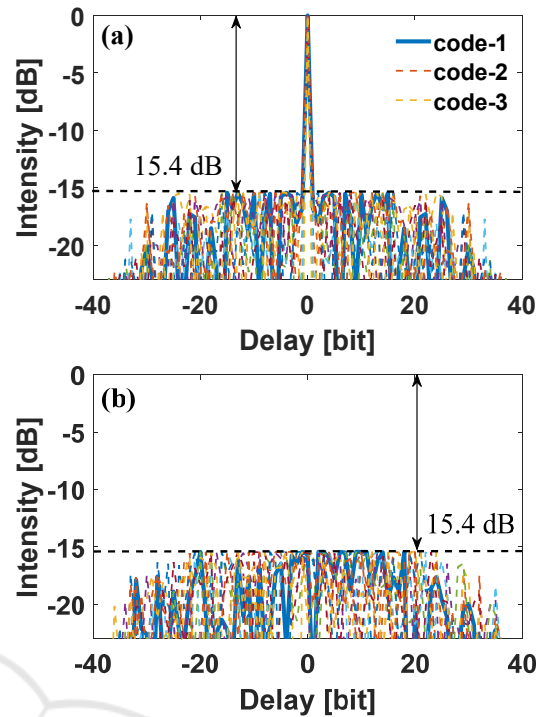


Figure 1: The auto-correlation (a) and cross-correlation (b) functions of the 10 generated codes.

algorithm, which can be realized by the mathematical software in practice. With iteration process, the minimized objective function t can be obtained, demonstrating the minimized auto-correlation functions and cross-correlation functions are realized.

Through the method above, ten groups of codes are successfully generated, and all of them have about 15.4 dB auto-correlation and cross-correlation suppression ratio, shown in Figure 1 (a) and (b) respectively.

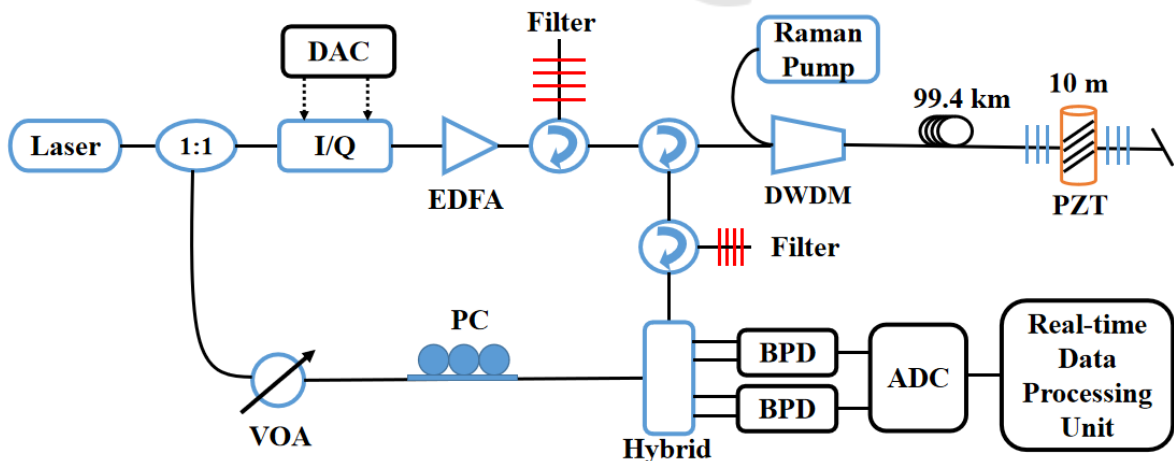


Figure 2: The experimental setup. I/Q: I/Q electro-optical modulator; EDFA: erbium-doped fiber amplifier; DWDM: dense wavelength division multiplexing modulator; VOA: variable optical attenuator; PC: polarization controller.

3 EXPERIMENTAL RESULTS

The experimental setup is shown in Figure 2. The lightwave is emitted from the laser (NKT X15) and the continuous lightwave from laser source is split into two branches equally by a polarization maintaining 1:1 coupler. The upper branch is the sensing arm, and the lower one is used as the local oscillator (LO).

The lightwaves in the sensing arm are modulated by the I/Q electro-optical modulator according to the codes generated above. All of the ten codes have a 400 MHz frequency shift, so that the heterodyne detection can be applied and every code is with 400 ns width. The modulated probe codes are amplified by the erbium-doped fiber amplifier (EDFA) and be filtered out by a tunable filter.

Then the probe signal is guided into the sensing section. The Raman shift in SMF is 13.2 THz, indicating that a pump light with a wavelength of 1455 nm has a large Raman gain at 1550 nm. Thus, to achieve the long distance fiber sensing, a 1455 nm Raman pump is used for distributed amplification. The probe signal and the pump signal are combined by the dense wavelength division multiplexing (DWDM) modulator to achieve amplification. Then the signals are guided into the sensing fiber, which is composed of a 99.4 km SMF and a pair of FBGs. The reflectivity of the FBGs is about -10 dB, and the interval between the two FBGs is 10 m. A variable optical attenuator (VOA) is added to the fiber line to compensate for the difference in fiber loss between SMF and FBGs. Besides, a piezoelectric ceramics transducer (PZT) is applied between two FBGs at the end of the fiber to simulate the external vibration.

The reflected signal from sensing fiber will be collected by the circulator and filtered out by a tunable filter. Then the signal is beat with the LO in an optical hybrid. The mixed lightwaves are detected by two balanced photodetectors (BPDs). Finally, the two-channel photoelectric-signals are sampled by a high speed analog to digital converter (ADC) with 3.2 GSa/s acquisition rate. By utilizing GPU parallel processing technology, the speed of computation can be greatly improved and the signal can be demodulated in real time.

In the conventional QDAS, the sensing bandwidth is limited by the pulse round-trip time in sensing fiber. The total length of the sensing distance is 99.4 km, representing 972.9 μ s round-trip time. The total repetition period is supposed to be a little longer than the round-trip time of the pulse. In practice, the interval between adjacent codes is 100 μ s, indicating that the total repetition period is 1 ms. The repetition

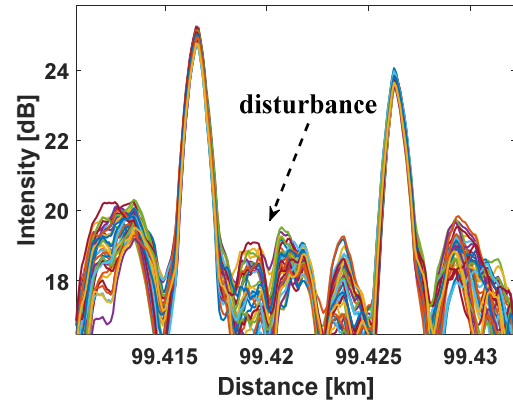


Figure 3: The intensity curves of the sensing signal.

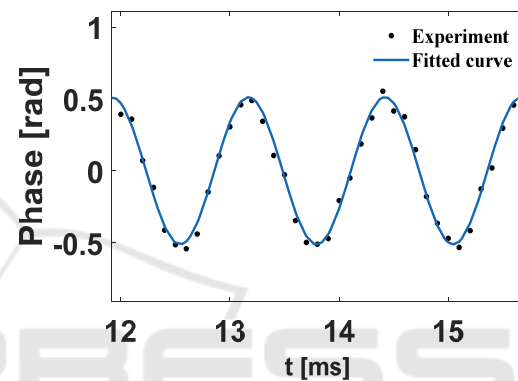


Figure 4: The measured 0.8 kHz sinusoidal signal.

period represents a 1 kHz scan-rate in the conventional QDAS system and according to the Nyquist sampling theorem, the sensing bandwidth of it is 500 Hz. By introducing the MIMO technology in QDAS, the scan-rate of the system is as high as 10 kHz, which is ten times of the maximum scan-rate in traditional single-pulse scheme, bounded by the 1 ms repetition period, and the sensing bandwidth is accordingly enlarged to 5 kHz.

A 800 Hz sinusoidal signal is applied on the PZT first to verify the sensing ability of MIMO-QDAS. The demodulated traces are plotted in Figure 3, and the reflected signals at each FBG are separated clearly, indicating the spatial resolution of 10 m is realized. The measured signal in real time is shown in Figure 4, the black dots are experimental results and the fitted curve of the measured signal is also plotted in blue, which is approximately a sinusoidal wave model, demonstrating the good sensing performance of the real-time MIMO-QDAS.

In order to verify the enlargement of the sensing bandwidth, sinusoidal signals of different frequencies are added on the PZT. The frequencies of the three signals are 1.2 kHz, 3.1 kHz and 4.9 kHz respectively.

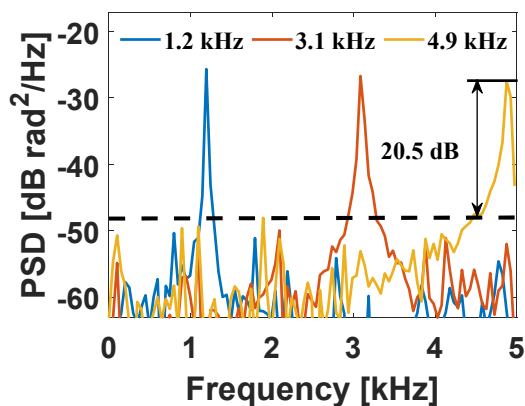


Figure 5: The PSD of the measured acoustic signals in different frequencies.

The power spectrum density (PSD) of the real-time demodulated signals are illustrated in Figure 5. The lowest SNR of the acoustic signals is 20.5 dB, which indicates that the real-time acoustic signals can be required with high quality clearly. The maximum noise level around the 4.9 kHz disturbance frequency is about -48.1 dB, and the strain noise level is $43.8 \text{ } \mu\epsilon/\sqrt{\text{Hz}}$.

4 CONCLUSIONS

In this paper, a real-time MIMO-QDAS with high performance is demonstrated by utilizing the OCSF. The generation of the codes is elaborated and ten groups of codes with about 15.4 dB auto-correlation and cross-correlation suppression ratio are obtained. As a result, the sensing bandwidth is enlarged to 5 kHz on 99.4 km sensing distance, which is ten times of that in the conventional QDAS without multiplexing and the spatial resolution is 10 m. The multiplexed channels are doubled compared with the previous MIMO-QDAS system that our group achieved, and real-time signal demodulation is demonstrated. Particularly, a 4.9 kHz sinusoidal strain signal is retrieved in real time, with $43.8 \text{ } \mu\epsilon/\sqrt{\text{Hz}}$ noise level.

ACKNOWLEDGEMENTS

National Natural Science Foundation of China (62075030); Sichuan Provincial Project for Outstanding Young Scholars in Science and Technology (2020JDJQ0024).

REFERENCES

- Ping Lu, Nageswara Lalam, Mudabbir Badar, Bo Liu, Benjamin T. Chorpening, Michael P. et al. (2019). "Distributed optical fiber sensing: Review and perspective", *Applied Physics Reviews* 6, 041302.
- Yaxi Yan, Hua Zheng, Zhiyong Zhao, Changjian Guo, Xiong Wu, Junhui Hu, Alan Pak Tao Lau, and Chao Lu. (2021). "Distributed Optical Fiber Sensing Assisted by Optical Communication Techniques" *J. Lightwave Technol.* 39, 3654-3670.
- L. Zhou, F. Wang, X. Wang, Y. Pan, Z. Sun, J. Hua, and X. Zhang. (2015). "Distributed Strain and Vibration Sensing System Based on Phase-Sensitive OTDR", *IEEE Photonics Technol. Lett.* 27(17), 1884-1887.
- J. Liang, Z. Wang, B. Lu, X. Wang, L. Li, Q. Ye, R. Qu, and H. Cai. (2019). "Distributed acoustic sensing for 2D and 3D acoustic source localization", *Opt. Lett.* 44(7), 1690-1693.
- Rao, Y., Wang, Z., Wu, H, Huijuan Wu, Zengling Ran, and Bing Han. (2021). "Recent Advances in Phase-Sensitive Optical Time Domain Reflectometry (Φ -OTDR)", *Photonic Sens* 11, 1-30.
- E. F. Williams, M. R. Fernández-Ruiz, R. Magalhaes, R. Vanthillo, Z. Zhan, M. González-Herráez, and H. F. Martins. (2019). "Distributed sensing of microseisms and teleseisms with submarine dark fibers", *Nat. Commun.* 10, 1-11.
- M.-F. Huang, M. Salemi, Y. Chen, J. Zhao, T. J. Xia, G. A. Wellbrock, Y.-K. Huang, G. Milione, E. Ip, P. Ji, T. Wang, and Y. Aono. (2020). "First field trial of distributed fiber optical sensing and high-speed communication over an operational telecom network", *J. Light. Technol.* 38, 75-81.
- M. Wu, X. Fan, Q. Liu, and Z. He. (2020). "Quasi-distributed fiber-optic acoustic sensing system based on pulse compression technique and phase-noise compensation", *Opt. Lett.*, vol. 44, no. 24, pp. 5969-5972.
- Z. Wang, B. Zhang, J. Xiong, Y. Fu, S. Lin, J. Jiang. et al. (2018). "Distributed acoustic sensing based on pulse-coding phase-sensitive OTDR", *IEEE Internet Things J.*, vol. 6, no. 4, pp. 6117-6124.
- X. Zhang, G. Zheng, Y. Shan, Z. Sun, and Y. Zhang. (2016). "Enhanced ϕ -OTDR system for quantitative strain measurement based on ultra-weak fiber Bragg grating array", *Opt. Eng.* 55, 054103.
- G. Liang, J. Jiang, K. Liu, S. Wang, T. Xu, W. Chen, Z. Ma, Z. Ding, X. Zhang, Y. Zhang, and T. Liu. (2020). "Phase demodulation method based on a dual-identical-chirped-pulse and weak fiber Bragg gratings for quasi-distributed acoustic sensing", *Photon. Res.* 8, 1093-1099.
- H. Li, Q. Sun, T. Liu, C. Fan, T. He, Z. Yan, D. Liu, and P. P. Shum. (2020). "Ultra-high sensitive quasi-distributed acoustic sensor based on coherent OTDR and cylindrical transducer", *J. Light. Technol.* 38, 929-938.
- B. Redding, M. J. Murray, A. Donko, M. Beresna, A. Masoudi, and G. Brambilla. (2020). "Low-noise

- distributed acoustic sensing using enhanced backscattering fiber with ultra-low-loss point reflectors*", Opt. Express 28, 14638–14647.
- K. Yüksel, J. Jason, E. B. Koal, M. Lopez-Amo, and M. Wuilpart. (2020). "An overview of the recent advances in FBG-assisted phase-sensitive OTDR technique and its applications," in Transparent Optical Networks, 2020. ICTON 2020.
- Zitan Wang, Jialin Jiang, Zinan Wang, Ji Xiong, Zijie Qiu, Chunye Liu, and Yunjiang Rao. (2020). "Quasi-distributed acoustic sensing with interleaved identical chirped pulses for multiplying the measurement slew-rate", Opt. Express 28, 38465–38479.
- L. Xin, Z. Li, X. Gui, X. Fu, M. Fan, J. Wang, and H. Wang. (2020). "Surface intrusion event identification for subway tunnels using ultra-weak FBG array based fiber sensing", Opt. Express 28(5), 6794–6805.
- W. Gan, S. Li, Z. Li, and L. Sun. (2019). "Identification of ground intrusion in underground structures based on distributed structural vibration detected by ultra-weak FBG sensing technology", Sensors 19(9), 2160.
- M. Wu, X. Fan, X. Zhang, L. Yan, and Z. He. (2020). "Frequency response enhancement of phase-sensitive OTDR for interrogating weak reflector array by using OFDM and vernier effect", J. Light. Technol. 38, 4874–4882.
- Z. Wang, J. Jiang, Z. Wang, J. Xiong, and Y.-J. Rao. (2020). "Bandwidth-enhanced quasi-distributed acoustic sensing with interleaved chirped pulses", IEEE Sensors J. 20, 12739–12743.
- Y. X. Zhang, S. Y. Fu, Y. S. Chen, Z. W. Ding, Y. Y. Shan, F. Wang, et al. (2019). "A visibility enhanced broadband phase-sensitive OTDR based on the UWFBG array and frequency-division-multiplexing", Opt. Fiber Technol. 53, 101995.
- J. Jiang, J. Xiong, Z. Wang, Z. Wang, Z. Qiu, C. Liu, Z. Deng, and Y.-J. Rao. (2021). "Quasi-distributed fiber-optic acoustic sensing with MIMO technology", in IEEE Internet of Things Journal, vol. 8, no. 20, pp. 15284–15291, 15 Oct.15.
- Jialin Jiang, Ziwen Deng, and Zinan Wang. (2021). "Channel-multiplexing for quasi-distributed acoustic sensing with orthogonal codes", Opt. Express 29, 36828–36839.
- Seong-Jung Kim, and Jeong-Hae Lee. (2018). "Resonance Frequency and Bandwidth of the Negative/Positive n th Mode of a Composite Right-/Left-Handed Transmission Line". J. Electromagn Eng Sci. 2018;18(1):1-6.
- J. Jiang, Z. Wang, Z. Wang, Y. Wu, S. Lin, J. Xiong, Y. Chen, and Y. Rao. (2019). "Coherent Kramers-Kronig receiver for Φ -OTDR," J. Lightwave Technol. 37(18), 4799–4807.
- Xiong J, Wang Z, Wu Y, Wu H, Rao Y. (2020). "Long-distance distributed acoustic sensing utilizing negative frequency band", Opt Express. 2020 Nov 23;28(24):35844–35856.
- Wang Z, Zhang L, Wang S, Xue N, Peng F, Fan M, Sun W, Qian X, Rao J, Rao Y. (2016). *Coherent Φ -OTDR based on I/Q demodulation and homodyne detection*. Opt Express. 24(2):853-8.
- Z. Q. Pan, K. Z. Liang, Q. Ye, et al. (2011). *Phase-sensitive OTDR system based on digital coherent detection*. Asia Communications and Photonics Conference and Exhibition, Shanghai, 2011: 83110S.
- W. Tomboza, S. Guerrier, E. Awwad and C. Dorize. (2021). "High Sensitivity Differential Phase OTDR for Acoustic Signals Detection", in IEEE Photonics Technology Letters, vol. 33, no. 13, pp. 645-648.
- D. Chen, Q. Liu, and Z. He. (2017). "Distributed Fiber-optic Acoustic Sensor with Sub-nano Strain Resolution Based on Time-gated Digital OFDR", in Asia Communications and Photonics Conference, OSA Technical Digest (Optical Society of America, 2017), paper S4A.2.
- Shuker R and Gammon RW. (1970). *Raman-scattering selection-rule breaking and the density of states in amorphous materials*. Phys Rev Lett 25:222–235.